

## Angle-resolved Andreev bound states in anisotropic $d$ -wave high- $T_c$ $\text{YBa}_2\text{Cu}_3\text{O}_{7-y}$ superconductors

I. Iguchi,<sup>1</sup> W. Wang,<sup>1</sup> M. Yamazaki,<sup>1</sup> Y. Tanaka,<sup>2</sup> and S. Kashiwaya<sup>3</sup>

<sup>1</sup>Department of Physics and CREST-JST, Tokyo Institute of Technology, Tokyo 152-8551, Japan

<sup>2</sup>Department of Applied Physics, Nagoya University, Nagoya 464-8603, Japan

<sup>3</sup>Electrotechnical Laboratory, Tsukuba 305-8568, Japan

(Received 12 June 2000)

An unusual technique utilizing the two-dimensional junction configuration is introduced to study the pairing symmetry of a  $\text{YBa}_2\text{Cu}_3\text{O}_{7-y}$  cuprate superconductor. The zero bias conductance peak due to the Andreev bound states was measured for the  $\text{YBa}_2\text{Cu}_3\text{O}_{7-y}/\text{I}/\text{Ag}$  ramp-edge tunnel junctions with different crystal-interface boundary angles fabricated on the same chip. It was found to develop monotonically as the angle was increased and became a maximum at  $45^\circ$ . Two gaplike structures were also found at the intermediate angle of  $30^\circ$ . The result implies that  $d_{x^2-y^2}$ -wave pairing symmetry predominates in this cuprate.

Considerable evidence exists showing that the hole-doped high- $T_c$  cuprate superconductors have  $d_{x^2-y^2}$ -wave pairing symmetry.<sup>1-4</sup> The order parameter is anisotropic, becomes zero along the nodes of a cylindrical Fermi surface, and changes sign in the orthogonal  $k$  directions. When an electron in the normal metal tunnels into an anisotropic superconductor, the injected quasiparticle experiences a different pair potential depending on the angle  $\alpha$  between the crystal orientation (e.g.,  $a$  axis) of the superconductor and the interface boundary [see Fig. 1(a)]. Due to the sign change of the  $d$ -wave order parameter, the quasiparticles form the bound states at the interface boundary, i.e., Andreev bound states (ABS).<sup>5</sup> The ABS appears as a zero bias conductance peak (ZBCP) in the tunnel conductance curve of a superconductor/insulator/normal metal (S/I/N) junction.<sup>6</sup> The ZBCP height depends on the angle  $\alpha$ , becoming the maximum at  $\alpha=45^\circ$  and zero at  $\alpha=0^\circ$ . Here we show an angle-resolved measurement on ABS using the  $\text{YBa}_2\text{Cu}_3\text{O}_{7-y}$  (YBCO)/I/Ag junctions with different angle  $\alpha$  fabricated on the same chip simultaneously. Our results strongly support the predominant  $d_{x^2-y^2}$ -wave symmetry.

The ZBCP for anisotropic high- $T_c$  superconductors has attracted considerable attention because it contains the information on the superconducting phase, similar to the Josephson effect. The experimental data provided a variety of results for ZBCP for the facets (100) ( $\alpha=0^\circ$ ), (110) ( $\alpha=45^\circ$ ), and (001) ( $c$  axis) using STM techniques or planar junctions.<sup>7-17</sup> For example, ZBCP has been observed for the (110) surface in almost all the measurements, while there are very few reports on its absence on the (100) surface. To explain the presence of ZBCP on the (100) surface, some people evoked the  $s$ -wave symmetry at microscopic faceting of the boundary due to the broken time reversal symmetry.<sup>11,17,18</sup> In the case of a planar junction, the contribution of the different facets due to the rough surface morphology might be naturally expected. No reports exist for an intermediate angle of  $0^\circ < \alpha < 45^\circ$ . For  $0^\circ < \alpha < 45^\circ$ , the monotonic increase of ZBCP with the increase of the angle  $\alpha$  should be observed, according to the recent theories of tunnel conductance for the  $d_{x^2-y^2}$  symmetry pairing.<sup>6,19</sup>

To clarify this situation, it is of vital importance to compare the ZBCP of high quality junctions with different angles  $\alpha$  fabricated under the same conditions. In this paper, we show the angle-resolved ZBCP measurement of the ramp-edge type YBCO/I/Ag junctions with various angles  $\alpha$  fabricated on the same chip, as shown in Figs. 1(b) and 1(c). The ramp-edge junction<sup>20,21</sup> has been considered to be the most promising junction for the application to superconducting electronics, such as rapid single flux quantum (RSFQ) circuits.<sup>22</sup> The ramp-edge technique allows us to fabricate the junctions at any arbitrary angle  $\alpha$ . The preliminary measurement yielded a reasonable result for the  $0^\circ$  and  $45^\circ$  ramp-edge junctions, but not for arbitrary angle  $\alpha$  because of the

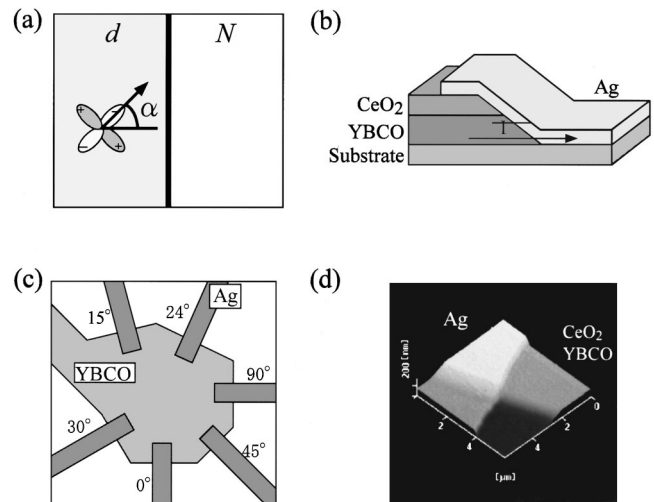


FIG. 1. (a) Schematic of a  $d$ -wave superconductor/normal metal junction, where  $\alpha$  is the angle between the crystal orientation of a superconductor and the line normal to the interface boundary. (b) Cross-sectional view of a ramp-edge junction geometry. The current  $I$  flows from an Ag metal into the  $ab$  plane of a YBCO superconductor. (c) Top view of the sample with six ramp-edge junctions with different angles. Note that the YBCO electrode is common to all junctions. (d) Atomic force microscope (AFM) image of the ramp-edge surface.

lack of a careful fabrication technique of the junctions of high quality.<sup>23</sup>

In the present measurements, we have fabricated six ramp-edge junctions by *in situ* deposition of YBCO and Ag films, photolithography, and Ar ion milling techniques on an MgO substrate, as described below [Fig. 1(b)]. High quality YBCO thin films were deposited by a pulsed laser deposition model. The  $T_c$ 's of the films were about 90 K with the transition width less than 3 K, and the thickness was 200 nm. The x-ray diffraction (XRD) pattern showed only pronounced *c*-axis (001)-oriented peaks. For the investigation of the perfection of the in-plane *ab* orientation, we employed the x-ray pole figure measurements. The pole figures were obtained by scanning the tilted angle of beam/detector from 0° to 90°. With fixing the detector angle  $2\theta$  at 32.84°, only four peaks corresponding to the reflection of (103) were observable. When  $2\theta$  was fixed at 58.20°, 12 peaks corresponding to 12 equivalent reflections of (116) for (100)-oriented YBCO were observable. The results confirm that the deposited YBCO film has an almost perfect in-plane orientation with the substrate crystal.

To fabricate the ramp-edge junction, we took special care for forming flat ramp-edge surfaces. After depositing the 150-nm-thick CeO<sub>2</sub> layer, the sample was set on a water-cooled rotatable holder and etched by Ar ion milling of a relatively small acceleration voltage of 250 V. During the ion milling process, the sample holder was rotated at the rate of 10 rpm, which was necessary for obtaining the junction uniformity suitable for the angle-resolved measurement.<sup>24</sup> To define the sharp edge structure, a photoresist treatment was also developed. After removal of photoresist, the surface was again cleaned by ion milling at 150 V. With this process, a highly flat edge with a slope angle of about 30° was formed, as shown in Fig. 1(d). *In situ* deposition of Ag after cleaning followed, and the sample was finally patterned to give the junction geometry, as shown in Fig. 1(b). Six junctions with different tilt angles  $\alpha=10^\circ, 15^\circ, 24^\circ, 30^\circ, 45^\circ$ , and  $90^\circ$  and the width of either 20  $\mu\text{m}$  or 50  $\mu\text{m}$  were fabricated simultaneously on the same substrate. The insulating barrier was natively grown. In most cases, the resistances of six junctions were about the same, typically of the order of  $10^{-5} \Omega \text{cm}^2$ . The measurements of the conductance vs voltage curves were carried out by the standard four-terminal method utilizing a lock-in amplifier.

The top figure in Fig. 2 shows the results on the angle-resolved conductance measurements for  $\alpha=0^\circ, 15^\circ, 24^\circ, 30^\circ$ , and  $45^\circ$  at 4.2 K. Noticeably, ZBCP grew continuously as the angle  $\alpha$  was increased with its maximum height at  $45^\circ$ . For the  $\alpha=90^\circ$  junction, the ZBCP became considerably small again, similar to that of  $\alpha=0^\circ$ . The appearance of very small ZBCP at  $\alpha=0^\circ$  and  $90^\circ$  might be attributed to possible crystal defects or a roughness effect on the edge surface. The bottom figure plotted the normalized ZBCP height (ZBCP height after background subtraction divided by the average gap-edge conductance) as a function of angle  $\alpha$  together with the curve expected for the  $d_{x^2-y^2}$ -wave symmetry. The data point at  $45^\circ$  indicates the corrected value after some factors are taken into account, as shown below. The agreement between the experiment and the theory is quite reasonable. For the  $d_{xy}$  symmetry, with increasing  $\alpha$ , the peak height is expected to decrease from its maximum value at  $\alpha=0^\circ$  to zero

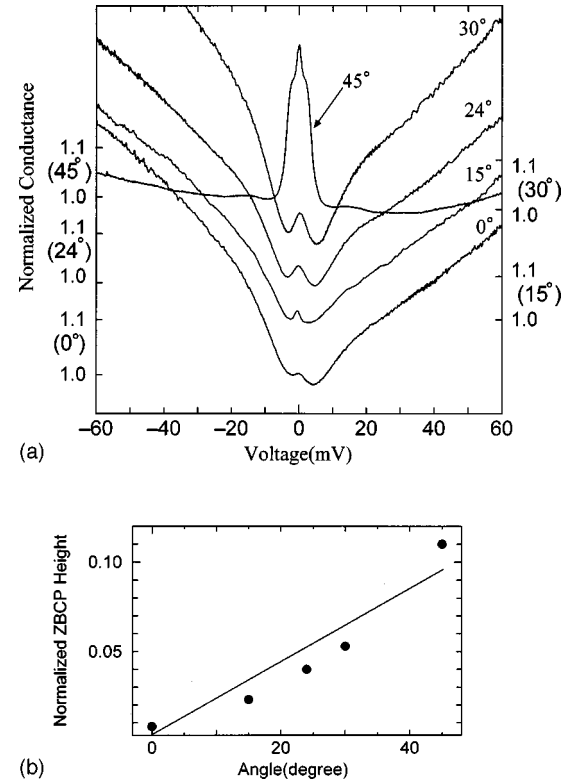


FIG. 2. Top: tunnel conductance curves as a function of junction voltage for the junctions with different orientation angles  $\alpha=0^\circ, 15^\circ, 24^\circ, 30^\circ,$  and  $45^\circ$ . For an eye guide, each conductance curve was shifted by a certain amount vertically. Bottom: normalized ZBCP height as a function of angle  $\alpha$ , together with the theoretical prediction. It is clearly observable that the zero bias conductance peak (ZBCP) increased from  $0^\circ$  [(100) orientation] continuously, as predicted by the tunneling calculation based on the  $d_{x^2-y^2}$ -wave theory (Ref. 19).

at  $\alpha=45^\circ$ . In the case in which the *s*-wave component is involved in the surface pairing symmetry, such as  $d_{x^2-y^2} + is$  symmetry, the different behavior should be expected.<sup>18,25</sup> For the extended *s*-wave symmetry, the ZBCP height becomes zero at  $\alpha=0^\circ$  and  $45^\circ$ , and takes the maximum value for the angles  $\alpha$  in between.<sup>26</sup> These predictions are inconsistent with our experimental observations.

The peak height at  $45^\circ$  appeared pronouncedly and the additional shoulder structures were observed. We interpret this in the following way. The theory predicts that the ZBCP height strongly depends on the magnitude of junction resistance and becomes greater for larger resistance. In this sample, the average junction resistances at the gap voltage for the junctions from  $0^\circ$  to  $30^\circ$  were almost the same, but it was about four times greater for the  $45^\circ$  junction, hence large ZBCP was observed. The flat conductance for the  $45^\circ$  junction is generally expected for the junctions with high resistance. The shoulder structures might be produced by the damage, probably due to the Ar ion milling process, creating some local oxygen nonstoichiometric region in the junction. Then we may deal with the two channel model, one intrinsic to the *d*-wave symmetry, the other characteristic of disordered crystal. The shoulders disappeared by applying a magnetic field of 1 T. Incidentally, the ZBCP height was reduced by 20% of that of the original peak. By considering the

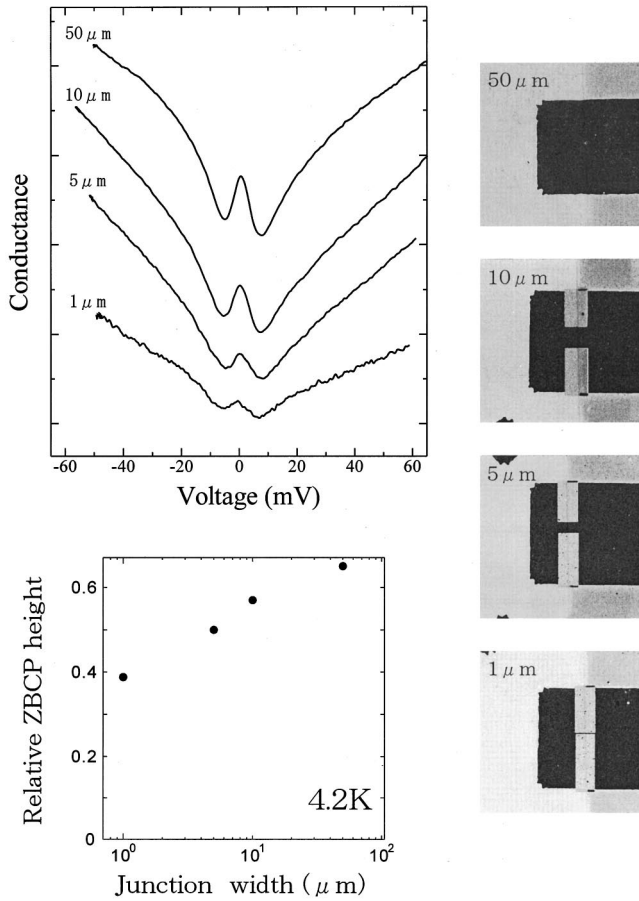


FIG. 3. Top left: tunnel conductance curves for the ramp-edge junctions with different widths. All data were taken from one specific ramp-edge junction originally having the width of 50  $\mu\text{m}$  and by reducing its width down to 1  $\mu\text{m}$  by a focused ion beam technique, subsequently, as shown in the right figure. Bottom: relative ZBCP height as a function of the junction width.

above factors, the normalized ZBCP height at 45° becomes comparable to the other ZBCP height, as shown in Fig. 2. With increasing temperature, all ZBCP's at various angles became smaller, approximately described by the  $1/T$  rule as given in Ref. 28.

While the junctions are considered to have high quality due to our careful fabrication technique, one should check whether the junctions are indeed quite uniform or not. To investigate this, we performed the following experiment. First, we measured the conductance characteristic of a junction of 50  $\mu\text{m}$  wide at 4.2 K. Next, using a focused-ion beam technique, we reduced its width to 10  $\mu\text{m}$  and thereafter performed the measurement at 4.2 K. We repeated this process from the width of 50  $\mu\text{m}$  down to 1  $\mu\text{m}$ . Such results are depicted in the top left figure of Fig. 3. The ZBCP observed for the junction of 50  $\mu\text{m}$  wide as also observable for the junction of 1  $\mu\text{m}$  wide. The conductance spectra appeared almost similar except that their absolute value changed two orders of magnitude due to the reduction of the junction width, demonstrating that the junctions were indeed quite uniform. Moreover, the measurements showed that the fabricated junctions were quite stable even under the ion beam irradiation and after several thermal cycles. The bottom figure in Fig. 3 shows the relative ZBCP height (ZBCP

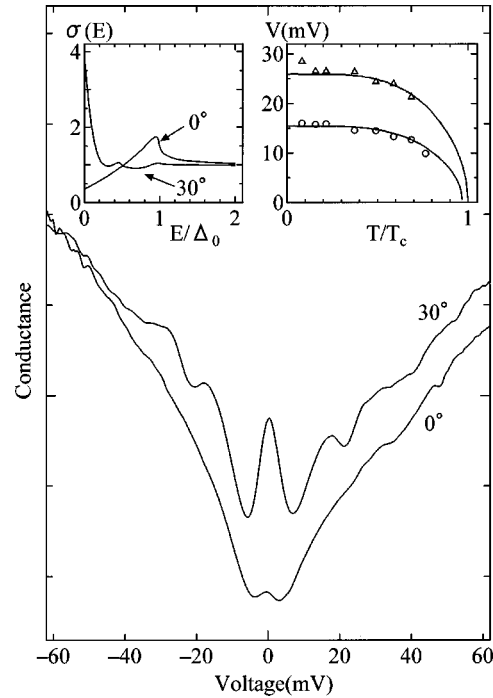


FIG. 4. Tunnel conductance curves for two junctions with  $\alpha=0^\circ$  and  $\alpha=30^\circ$  for which the gap structures appear rather clearly, together with the calculated results for the same angles based on the  $d_{x^2-y^2}$ -wave theory. For a guide to the eye, two conductance curves were shifted vertically with each other. Note that while one smeared gap-edge structure was observable for the  $0^\circ$  junction, two gaplike structures were observable for the  $30^\circ$  junction, suggesting the generation of an inner gap state or another Andreev bound state, in good qualitative agreement with the theoretical prediction. The temperature dependence of the gaplike structures exhibited a BCS-like behavior, as shown in the right inset.

height divided by the average gap-edge conductance after background subtraction) as a function of the junction width. As the width was reduced, the ZBCP height decreased, indicating that it becomes difficult for the Andreev reflection to occur. The result is consistent with the statement that the Andreev reflection will be completely suppressed in the limit of quantum wire.<sup>27</sup>

Figure 4 shows the example of a different sample for which the gap characteristics appeared more closely. Two conductance curves correspond to the junctions with  $\alpha=0^\circ$  and  $\alpha=30^\circ$ . While one gap-edge structure is observable for the  $\alpha=0^\circ$  junction, two gaplike structures are visible for the  $\alpha=30^\circ$  junction, one at  $V=25$  mV, the other at  $V=15$  mV. The detailed calculations on the  $d$ -wave conductance curves at the intermediate angles  $\alpha$  have been performed by Barash *et al.*<sup>28</sup> and Buchholtz *et al.*,<sup>29</sup> for the case in which the barrier height is very high. Because of a small barrier height in our samples, we have recalculated the conductance characteristics from Ref. 6 by taking the spatial dependent effect into account. The inset shows such calculated results for  $\alpha=0^\circ$  and  $30^\circ$ . While only one gap edge structure is present for  $\alpha=0^\circ$ , two gaplike structures are visible for  $\alpha=30^\circ$ . This means that the second inner gap state or another ABS appears for this angle. The experimental results are generally in good qualitative agreement with the calculated ones, although more fine structures are seen. The temperature depen-

dence of the two gaplike structures for the  $\alpha=30^\circ$  junction is also given in the right inset, showing the good agreement with the BCS curve. Theoretically, two gaplike structures appear for the angle from about  $30^\circ$  to just below  $45^\circ$ , also consistent with our observations. On the other hand, Golubov and Kupriyanov<sup>30</sup> recently calculated the effect of rough interfaces because the quasiparticle reflection from the realistic interfaces is diffusive rather than specular. In this case, due to strong scattering in the interlayer, the  $d$ -wave component is reduced and the  $s$ -wave component is generated, resulting in the appearance of modulated structures in the density of states. The calculated results also show qualitative agreement with the observed conductance curves, including the Andreev bound states at finite voltages and the additional fine structures, although some parameters (angle  $\alpha$ , temperature  $T$ ) of the calculated results do not directly correspond to those of experimental observation. However,

looking at Fig. 2 and Fig. 4, it seems probable that the surface of an individual sample depends on the details of the microfabrication process or electromigration or contamination. In some cases, the  $s$  component is possibly induced. The smeared gap edges are common to almost all YBCO junctions reported previously, which may be probably associated with the short quasiparticle lifetime or the impurities in YBCO material. The appearance of slight ZBCP at  $\alpha=0^\circ$  might be again due to some crystal defect or the roughness effect.

The angle-resolved measurement of ZBCP using the high quality YBCO/I/Ag ramp-edge junctions fabricated on the same chip simultaneously yielded clear evidence of  $d_{x^2-y^2}$ -wave symmetry for a YBCO superconductor.

This work has been supported by CREST (Core Research for Evolutional Science and Technology) of the Japan Science and Technology Corporation (JST).

- 
- <sup>1</sup>D. J. Van Harlingen, *Rev. Mod. Phys.* **67**, 515 (1995), and references therein.
- <sup>2</sup>M. Sigrist and T. M. Rice, *Rev. Mod. Phys.* **67**, 503 (1995).
- <sup>3</sup>I. Iguchi, *Coherence in High Temperature Superconductors*, edited by G. Deutscher and A. Revcolevschi (World Scientific, Singapore, 1996), pp. 354–370, and references therein.
- <sup>4</sup>J. Annett, N. Goldenfeld, and A. Leggett, *Physical Properties of High Temperature Superconductors*, edited by D. M. Ginsberg (World Scientific, Singapore, 1996), Vol. 5.
- <sup>5</sup>C. R. Hu, *Phys. Rev. Lett.* **72**, 1526 (1994); *Phys. Rev. B* **57**, 1266 (1998).
- <sup>6</sup>Y. Tanaka and S. Kashiwaya, *Phys. Rev. Lett.* **74**, 3451 (1995).
- <sup>7</sup>J. Geerk, X. X. Xi, and G. Linker, *Z. Phys. B: Condens. Matter* **73**, 329 (1988).
- <sup>8</sup>M. Furuyama *et al.*, *Jpn. J. Appl. Phys., Part 2* **29**, L459 (1990).
- <sup>9</sup>I. Iguchi *et al.*, *Jpn. J. Appl. Phys., Part 2* **29**, L614 (1990).
- <sup>10</sup>J. H. Leseur, L. H. Green, W. L. Feldman, and A. Inam, *Physica C* **191**, 325 (1992).
- <sup>11</sup>M. Convington *et al.*, *Phys. Rev. Lett.* **79**, 277 (1997).
- <sup>12</sup>J. Y. T. Wei, N.-C. Yeh, D. F. Garrigus, and M. Strasik, *Phys. Rev. Lett.* **81**, 2542 (1998).
- <sup>13</sup>S. Sinha and K.-W. Ng, *Phys. Rev. Lett.* **80**, 1296 (1998).
- <sup>14</sup>L. Alff *et al.*, *Phys. Rev. B* **55**, 14 757 (1997).
- <sup>15</sup>S. Kashiwaya, Y. Tanaka, H. Takashima, Y. Koyanagi, and K. Kajimura, *Phys. Rev. B* **51**, 1350 (1995).
- <sup>16</sup>L. Alff *et al.*, *Eur. Phys. J. B* **5**, 423 (1998), and references therein.
- <sup>17</sup>Y. Tanuma, Y. Tanaka, M. Yamashiro, and S. Kashiwaya, *Phys. Rev. B* **57**, 7997 (1998).
- <sup>18</sup>M. Fogelstrom, D. Rainer, and J. Sauls, *Phys. Rev. Lett.* **79**, 281 (1997).
- <sup>19</sup>S. Kashiwaya, Y. Tanaka, M. Koyanagi, and K. Kajimura, *Phys. Rev. B* **53**, 2667 (1996).
- <sup>20</sup>J. Gao *et al.*, *J. Appl. Phys.* **72**, 1 (1992).
- <sup>21</sup>C. Horstmann *et al.*, *IEEE Trans. Appl. Supercond.* **2**, 2844 (1997).
- <sup>22</sup>K. K. Likharev and V. K. Semenov, *IEEE Trans. Appl. Supercond.* **1**, 1 (1991).
- <sup>23</sup>W. Wang, M. Yamazaki, K. Lee, and I. Iguchi, *Phys. Rev. B* **60**, 4272 (1999).
- <sup>24</sup>In Ref. 23, the sample holder was rotatable only by manual operation. Hence the ion milling was done by setting a sample holder at a fixed angle. This method proved not to yield a good result for the angle-resolved measurement in detail probably due to the junction nonuniformity in a microscopic scale. The continuous rotation of the sample holder was found to be essential for obtaining a good result. The optimum rotation frequency was found to be 10 rpm.
- <sup>25</sup>M. Matsumoto and H. Shiba, *J. Phys. Soc. Jpn.* **64**, 3384 (1995).
- <sup>26</sup>Y. Tanaka, *Coherence in High Temperature Superconductors*, edited by G. Deutscher and A. Revcolevschi (World Scientific, Singapore, 1996), pp. 393–413.
- <sup>27</sup>Y. Takagaki and K. H. Ploog, *Phys. Rev. B* **60**, 9750 (1999).
- <sup>28</sup>Y. S. Barash, A. A. Svidzinsky, and H. Burkhardt, *Phys. Rev. B* **55**, 15 282 (1997).
- <sup>29</sup>L. J. Buchholtz, M. Palumbo, D. Rainer, and J. A. Sauls, *J. Low Temp. Phys.* **101**, 1097 (1995).
- <sup>30</sup>A. A. Golubov and M. Yu. Kupriyanov, *IEEE Trans. Appl. Supercond.* **9**, 3444 (1999).